# Red Phosphorescence from Benzo[2,1,3]thiadiazoles at Room Temperature

Gregory D. Gutierrez,[†] Graham T. Sazama,[†] Tony Wu,[‡] Marc A. Baldo,[‡] and Timothy M. Swager*,[†]

[†]Department of Chemistry and [‡]Department of Electrical Engineering and Computer Science, Massachusetts Institute of Technology, Cambridge, Massachusetts 02139, United States

S *Supporting Information*

ABSTRACT: We describe the red phosphorescence exhibited by a class of structurally simple benzo[2,1,3]thiadiazoles at room temperature. The photophysical properties of these molecules in deoxygenated cyclohexane, including their absorption spectra, steady-state photoluminescence and excitation spectra, and phosphorescence lifetimes, are presented. Time-dependent density functional theory calculations were carried out to better understand the electronic excited states of these benzo[2,1,3]thiadiazoles and why they are capable of phosphorescence.
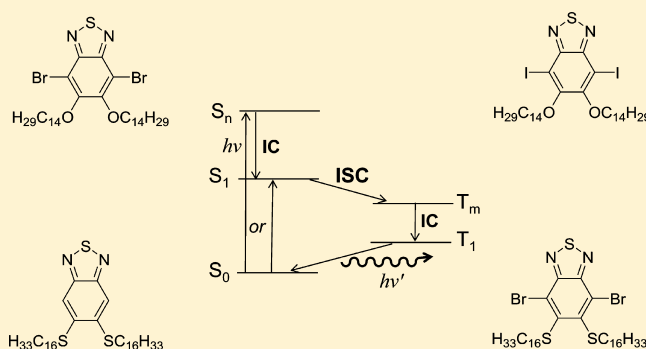
INTRODUCTION

Molecules capable of phosphorescence at room temperature have been utilized in a variety of technologies, most notably in light-emitting diodes (LEDs) for next-generation electronic displays.[1,2] Organometallic complexes containing platinum or iridium are often bright phosphorescent emitters because spin-orbit coupling induced by these heavy metal atoms bypass the quantum mechanical restrictions that prevent intersystem crossing (ISC) from occurring.[3] Nonmetalated organic molecules are also capable of ISC and are commonly investigated as triplet photosensitizers.[4] However, other classes of such materials may also produce phosphorescence at room temperature. For example, phosphorescent emission under ambient conditions has been observed from organic molecules dispersed in polymeric hosts[5−9] and zeolites[10] and various classes of nonmetalated solids, including halogenated benzophenones[11] and benzaldehydes,[12,13] carbazole-containing materials,[14,15] naphthalene diimides,[16] persulfurated aromatics,[17−19] and tellurophenes.[20,21] However, observing measurable phosphorescence from metal-free organic molecules dissolved in liquids at room temperature is often a challenging feat due to rapid nonradiative dissipation of a triplet state's energy under these conditions. As a result, few non-metalated organic molecules are known to produce significant phosphorescence in solution at room temperature.[22−25]

Benzo[2,1,3]thiadiazoles constitute a category of hetero-aromatic molecules that are widely used in the development of fluorescent π-conjugated organic materials.[26] We herein present the room-temperature red phosphorescence exhibited by four benzo[2,1,3]thiadiazoles in cyclohexane and describe their corresponding excited-state electronic properties using computational methods.

RESULTS AND DISCUSSION

Our study was prompted by the observation of room-temperature phosphorescence from 4,7-dibromo-5,6-bis-(tetradecyloxy)benzo[2,1,3]thiadiazole (**1-Br**, Figure 1a) and 4,7-diiodo-5,6-bis(tetradecyloxy)benzo[2,1,3]thiadiazole (**1-I**, Figure 1d), both of which are heteroaromatic linkers our laboratory has used to construct fluorescent semiconducting polymers.[27,28] The absorption spectra of these two molecules in cyclohexane at 50 μM are primarily confined to the ultraviolet region, and under aerobic conditions these solutions exhibit extremely weak blue fluorescence when excited at λ_{ex} = 370 nm. However, after deoxygenation with N_2 gas, **1-Br** and **1-I** demonstrate profoundly red-shifted emission maxima at λ_{max} = 642 nm and λ_{max} = 643 nm, respectively (Figures 1b and 1e). We assigned these unexpected red emissions as phosphorescence[29] as a result of the large downconversions of absorbed energy that results from ISC as well as the oxygen quenching of the long-lived triplet states. The phosphorescence quantum yields (Φ_P) of **1-Br** and **1-I** in degassed cyclohexane are 0.55% and 0.59%, respectively. Excitation spectra monitored at λ_{em} = 575 nm confirm that phosphorescence originates from **1-Br** and **1-I** by matching the structure of their corresponding absorption spectra (Figures 1c and 1f).

Because phosphorescence requires molecules to undergo ISC, the resulting photoluminescence lifetimes (τ_P) often occur on microsecond or millisecond time scales. Time-dependent transient photoluminescence spectroscopy was employed to determine if deoxygenated solutions of **1-Br** and **1-I** in
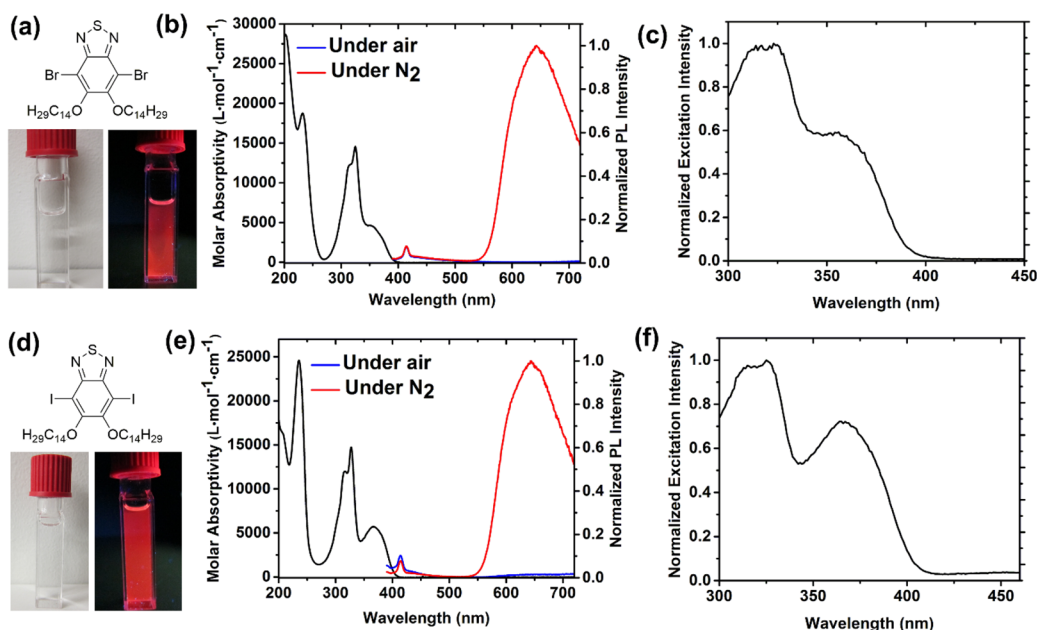
Figure 1. Photophysical properties of phosphorescent compounds **1-Br** and **1-I** in cyclohexane: (a) **1-Br** and (d) **1-I** and their appearance in degassed cyclohexane under normal and UV ($\lambda = 365$ nm) lighting; (b) absorption spectrum and photoluminescence spectra under air and N_2 gas for **1-Br** and (e) **1-I** ($\lambda_{ex} = 370$ nm); (c) phosphorescence excitation spectrum of **1-Br** and (f) **1-I** ($\lambda_{em} = 575$ nm). Photoluminescence and excitation spectra were measured for 50 μM solutions. A small peak attributed to Raman scattering ($\lambda_{max} = 414$ nm) of the excitation beam by the solvent overlaps with the fluorescence of all phosphorescent samples presented in this study and is not considered in our analysis.
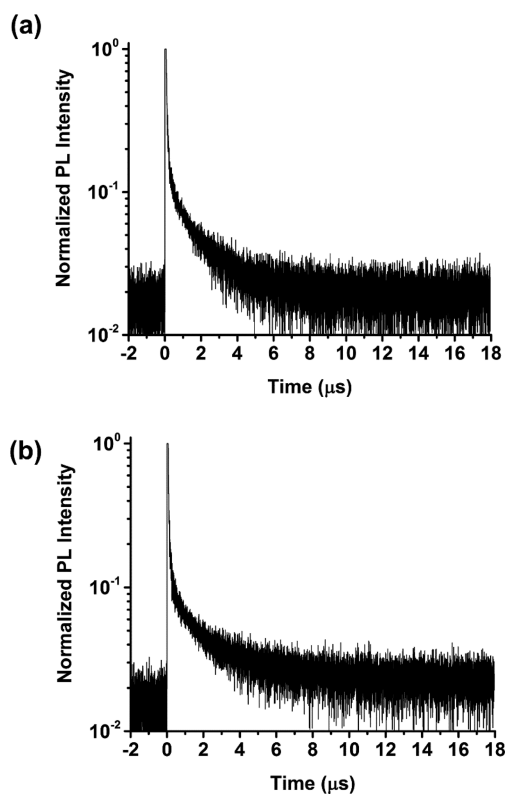

Figure 2. Time-dependent photoluminescence decays of (a) **1-Br** and (b) **1-I** in cyclohexane (50 μM) under inert atmosphere and at room temperature.

cyclohexane possess such long lifetimes. Under these conditions, the photoluminescence of each sample undergoes a mono-exponential decay on a microsecond-time scale (Figure 2). By fitting the intensities of the delayed responses to a first-order

kinetic model with respect to time, the data reveal that **1-Br** and **1-I** possess τ_P of 2.8 and 3.6 μs, respectively.

Following these results, we hypothesized that **1-Br** and **1-I** may be undergoing ISC and phosphorescence as a result of the influence of the heavy halides on their electronic properties. To investigate this possibility, we synthesized dichloride **1-Cl** and examined its photophysical properties in cyclohexane. **1-Cl** was accessed by reacting 5,6-bis(tetradecyloxy)benzo[2,1,3]-thiadiazole with *N*-chlorosuccinimide in the presence of iron(III) chloride (Scheme 1). Although it possesses an absorption spectrum

Scheme 1. Synthesis of Chlorinated Benzo[2,1,3]thiadiazole 1-Cl
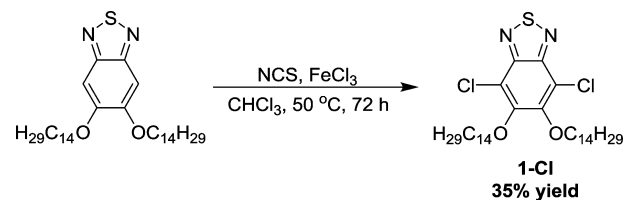
similar to those of **1-Br** and **1-I**, **1-Cl** primarily demonstrates blue fluorescence at $\lambda_{max} = 424$ nm with almost no red emission under deoxygenated conditions (Figure 3). Our results support the possibility that phosphorescence is facilitated by a heavy atom effect induced by the bromides and iodides in **1-Br** and **1-I**, respectively (see Calculations).

We next investigated if previously unreported benzo[2,1,3]-thiadiazoles are also phosphorescent. In particular, we prepared the molecules 5,6-bis(hexadecylthio)benzo[2,1,3]thiadiazole (**2-H**)[30] and 4,7-dibromo-5,6-bis(hexadecylthio)benzo[2,1,3]-thiadiazole (**2-Br**), the syntheses of which are presented in Scheme 2. To construct **2-H**, 2 equiv of 1-hexadecanethiol were directly coupled with 5,6-dibromobenzo[2,1,3]thiadiazole using the palladium-catalyzed methodology developed by Itoh
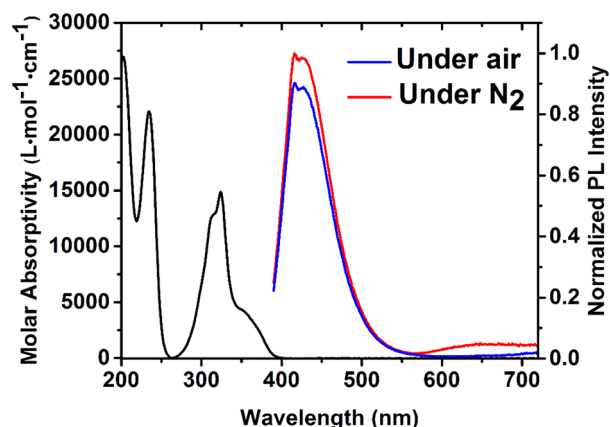
Figure 3. Absorption and emission spectra of **1-Cl** in cyclohexane. Emission spectra (λ_{ex} = 370 nm) are reported for 50 μM samples in aerobic and deoxygenated cyclohexane.

and Mase.[31] **2-Br** was subsequently synthesized via iodine-catalyzed bromination of **2-H**.

The absorption and photoluminescence spectra of 50 μM solutions of **2-H** and **2-Br** in cyclohexane are displayed in Figure 4b,e. The solutions of **2-H** and **2-Br** absorb only in the UV and blue regions but produce red emissions after deoxygenation with N$_2$ gas. **2-H** and **2-Br** thus demonstrate phosphorescence with maxima at λ_{max} = 624 nm and λ_{max} = 667 nm, respectively, with corresponding excitation spectra resembling their absorption profiles (Figure 4c,f). In the case of **2-H**, the excitation spectrum fully matches its absorption spectrum at much lower concentrations (i.e., 2.6 μM), an observation which is most likely the result of an inner-filter effect occurring at 50 μM. Both molecules also possess values of Φ_P similar to those of **1-Br** and **1-I** (0.70% for **2-H** and 0.50% for **2-Br**) in cyclohexane. Transient photoluminescence data indicate that τ_P is 5.4 μs for **2-H** and 3.4 μs for **2-Br** (Figures 4g,h). A summary of the photophysical properties of the four phosphorescent molecules described thus far is presented in Table 1.

■ CALCULATIONS

We next performed a computational analysis of the electronic excited states of the studied benzo[2,1,3]thiadiazoles in order to determine potential phosphorescence pathways. After ground state geometry optimization of model structures **1-Cl***, **1-Br***, and **1-I***, for which the large tetradecyloxy groups are replaced with propoxy substituents for computational efficiency, we carried out time-dependent density functional theory (TD-DFT) calculations to determine a mechanism for ISC. Throughout our analysis, we assume that internal conversion to S$_1$ always occurs prior to ISC (Kasha's rule).[33] For each molecule, two triplet states (T$_1$ and T$_2$) lie below the energy level of S$_1$ and thus provide thermodynamically favorable routes for ISC (Figure 5a). We subsequently characterized the excited states of the molecules using Kohn−Sham orbitals to depict the electronic configurational descriptions of the S$_1$, T$_1$, and T$_2$ states of each molecule (Figure 5b). We observe that, in all three molecules, the S$_1$, T$_1$, and T$_2$ states can all be described as symmetric $\pi \rightarrow \pi^*$ configurations. S$_1$ and T$_1$ are ≥88% described by a HOMO → LUMO configuration, while T$_2$ corresponds to a HOMO-1 → LUMO configuration (≥85% character). Because the transition symmetry of S$_1$ does not change during conversion to one of the lower-energy triplet states, ISC is most likely to be an inefficient process unless perturbations from one or more heavy atoms are introduced.[34] We conclude that ISC from S$_1$ to T$_2$ or T$_1$ could be facilitated by the heavy bromides and iodides through second-order perturbations such as a spin-orbit-vibronic interaction.[35] The lighter chlorides of **1-Cl*** likely do not carry a large enough atomic number to enable ISC in this manner, which explains why fluorescence dominates the photoluminescence spectrum of **1-Cl**.

Figure 6 displays the excited-state energy level diagrams for **2-H*** and **2-Br***, model systems where the long alkyl chains of the thioethers have been replaced with propyl groups (Figure 6a).[36] The corresponding Kohn−Sham orbitals for S$_1$, T$_1$, and T$_2$ are shown in Figure 6b. Unlike the other phosphors, **2-H** does not possess heavy halides that can enable ISC. However, the S$_1$ transition of **2-H*** is an (n,π^*) state in which most of the orbital density is concentrated at the sulfur atoms of the alkylthio groups. T$_1$ is best represented as a (π,π^*) state composed of a linear combination of configurations of HOMO-1 → LUMO (49% (π,π^*) character) and HOMO-2 → LUMO (44% (n,π^*) character). T$_2$, on the other hand, is a mix of mostly an (n,π^*) state with minority (π,π^*) character represented by two configurations: HOMO → LUMO (81% (n,π^*) character) and HOMO-3 → LUMO (15% (π,π^*)

Scheme 2. Syntheses of Thioether-Functionalized Benzo[2,1,3]thiadiazoles 2-H (a) and 2-Br (b)
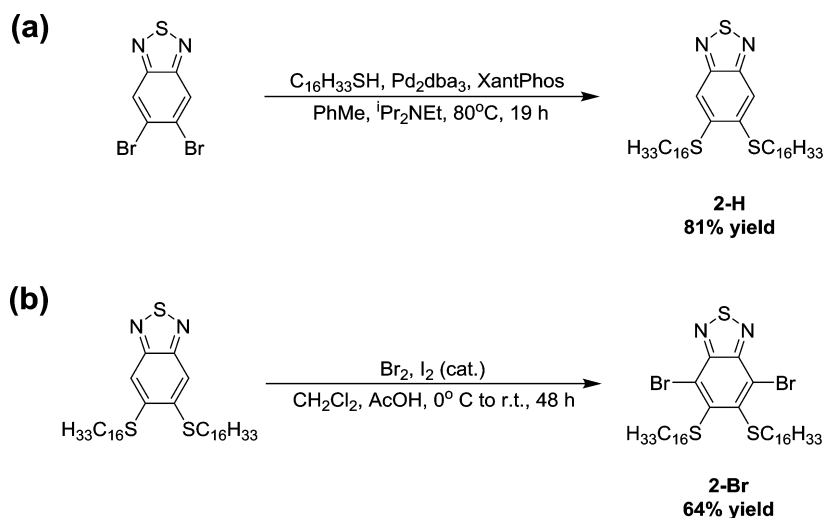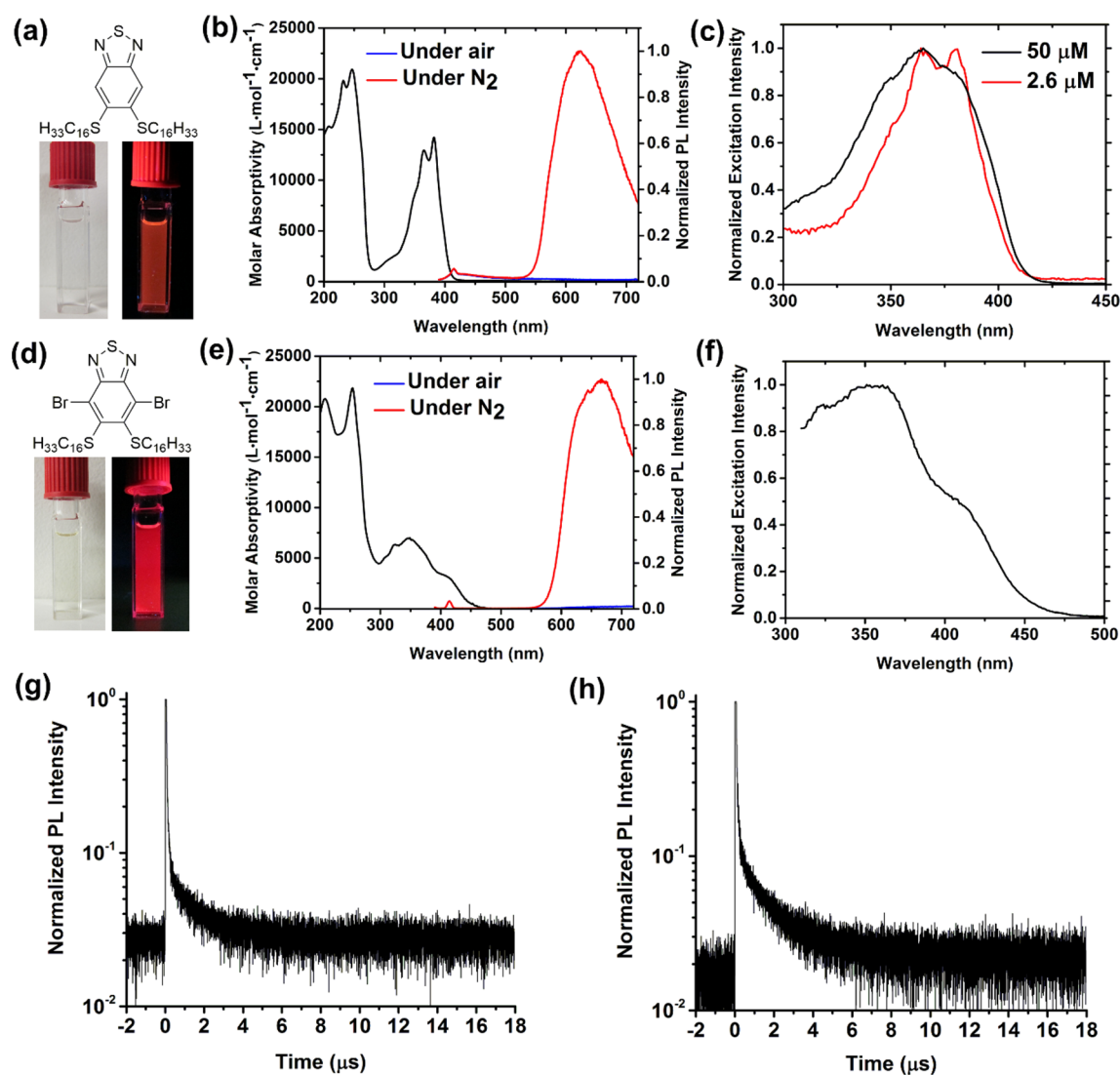
Figure 4. (a) **2-H** in cyclohexane with its (b) absorption spectrum and photoluminescence spectra under air and N_2 gas and (c) phosphorescence excitation spectra at 50 μM and 2.6 μM (λ_{em} = 575 nm). (d−f) **2-Br** with its corresponding absorption/photoluminescence spectra (λ_{ex} = 370 nm, 50 μM) and phosphorescence excitation spectrum (λ_{em} = 600 nm, 50 μM). (g) Time-dependent photoluminescence decays for **2-H** and (h) **2-Br** in deoxygenated cyclohexane at 50 μM.

Table 1. Summary of Photophysical Properties of Phosphorescent Benzo[2,1,3]thiadiazoles in Deoxygenated Cyclohexane

entry	$\lambda_{abs,max}$,[a] $\lambda_{em,max}$ (nm)	τ_P (μs)	Φ_P[b] (%)
1-Br	325, 642	2.8	0.55
1-I	327, 643	3.6	0.59
2-H	382, 624	5.4	0.70
2-Br	347, 667	3.4	0.50

[a]Absorption maximum past λ = 300 nm. [b]Measured at λ_{ex} = 370 nm using 9,10-diphenylanthracene in cyclohexane under air as a standard (Φ_{PL} = 77%).[32]

character). In this case, ISC is most likely possible by coupling a change in the spin angular momentum of the excited-state electron with the difference in the transition symmetries of the S_1 and T_1 manifolds (El-Sayed's rule).[37] Similarly, S_1 of **2-Br*** is an (n,π*) state,[38] whereas T_1 is a (π,π*) state and T_2 is mostly (n,π*). Thus, we conclude that a difference in angular orbital momentum between excited states can also lead to ISC.

CONCLUSION

To conclude, we have presented a set of structurally simple benzo[2,1,3]thiadiazoles with unusual phosphorescent emissions at room temperature. The rare solution-phase photophysical properties of these species provide a new direction aimed at uncovering new classes of metal-free organic phosphorescent materials. We are currently seeking to discover new molecular motifs and realize their potential as the active components of inexpensive LEDs and other optoelectronic technologies.

EXPERIMENTAL SECTION

Materials and Instrumentation. Unless otherwise stated, all solvents and reagents were used as purchased. Anhydrous toluene was obtained from a solvent purification system and stored over activated 3 Å molecular sieves. HPLC-grade cyclohexane was the solvent in all photophysical studies. 5,6-dibromobenzo[2,1,3]thiadiazole was purchased from TCI Chemical Co. and used without further purification. **1-I** was synthesized according to a literature procedure.[28] Column chromatography was carried out using silica gel (60 Å pore size, 230−400 mesh), and thin-layer chromatography (TLC) was performed with silica gel TLC plates. NMR spectra ([1]H: 400 MHz, [13]C: 101 MHz) were
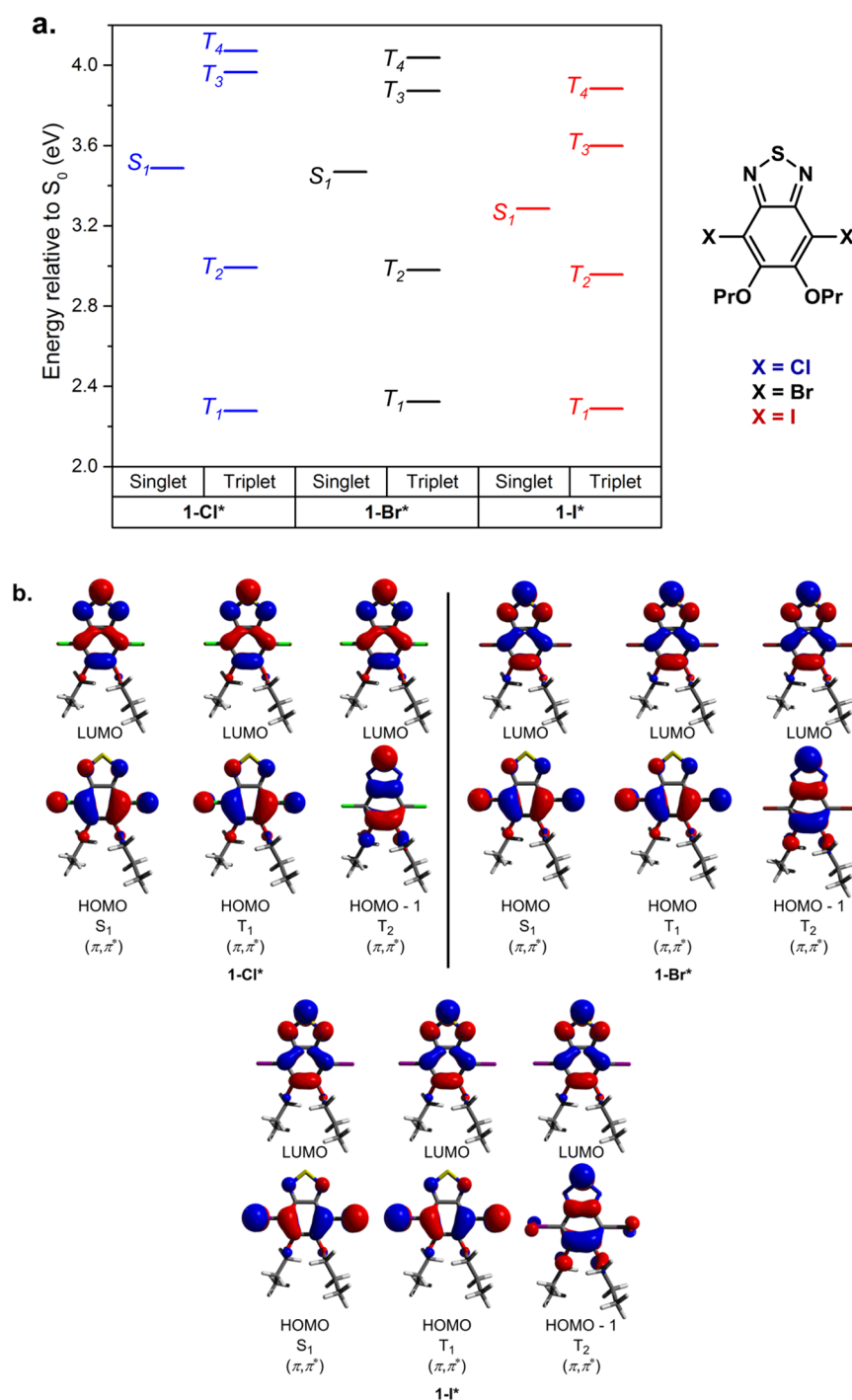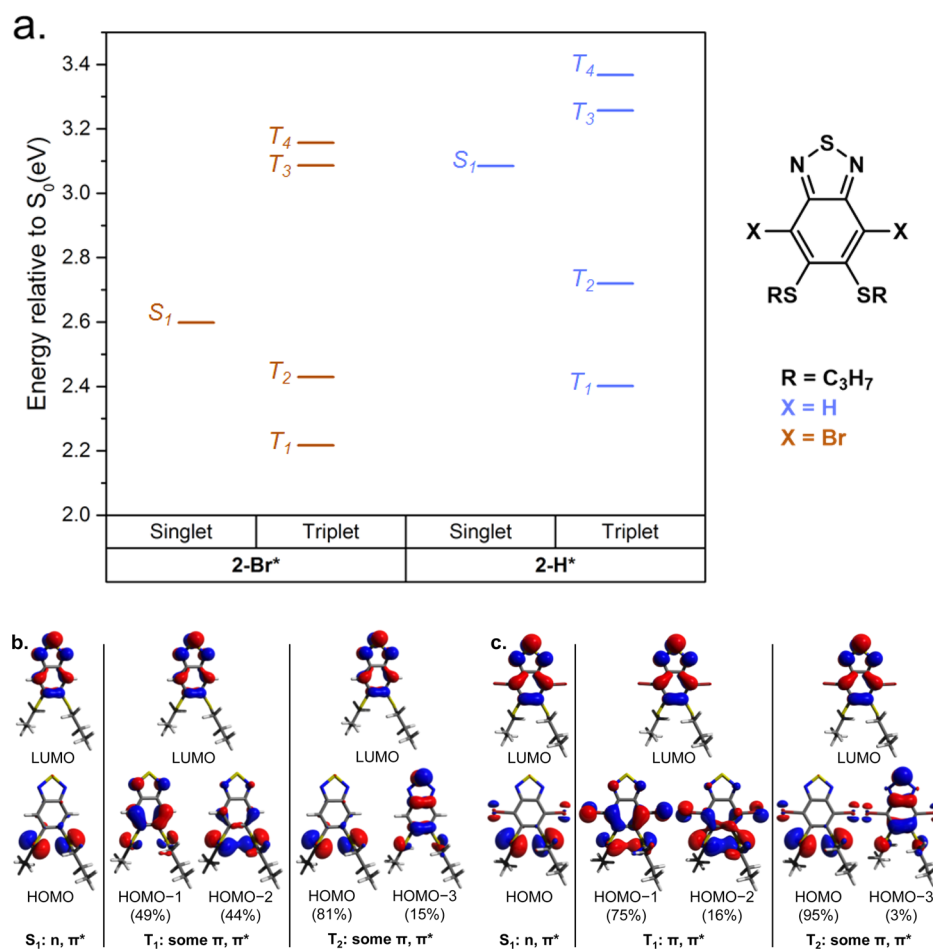
Figure 5. (a) Energy level diagrams for propoxy-functionalized derivatives **1-Cl***, **1-Br***, and **1-I*** in the gas phase. (b) Kohn–Sham orbitals representing the electronic configuration descriptions of S_1, T_1, and T_2 for each calculated molecule.

obtained with $CDCl_3$ as the solvent and were referenced relative to resonances corresponding to $CDCl_3$ (^1H: δ = 7.26 ppm; ^{13}C: δ = 77.16 ppm). NMR spectra were referenced relative to resonances corresponding to the solvent (^1H: δ = 7.26 ppm; ^{13}C: δ = 77.16 ppm). Peak multiplicities are designated as singlet ("s"), triplet ("t"), or multiplet ("m"). High-resolution mass spectrometry (HRMS) measurements were carried out in direct analysis in real time (DART) or with electrospray ionization (ESI) in positive mode using a Fourier transform-ion cyclotron resonance mass spectrometer.

All absorption spectra were measured with a UV/vis spectrophotometer under aerobic conditions. Photoluminescence spectra and excitation spectra were obtained with a spectrofluorometer employing a 450 W xenon short-arc lamp. Excitation and emission bandpass slits were set at 3 and 5 nm, respectively, and data were acquired with the excitation beam and detector oriented at a right angle. Photoluminescence spectra were corrected to account for wavelength-dependent responses by the detector, while excitation spectra were referenced relative to variations in the lamp intensity with wavelength. Phosphorescence quantum yields were measured using the relative method suggested by Brouwer[39] with all absorbances at the excitation wavelength maintained below 0.05 to prevent inner-filter effects from occurring. For these photoluminescence measurements, screw-top quartz cuvettes covered with a septum cap were used to hold solutions and were deoxygenated by purging them with N_2 gas for about 10 min to induce phosphorescence. For best results, solutions analyzed by spectroscopy were not exposed to UV radiation during the deoxygenation process.

Figure 6. (a) Energy level diagrams for **2-H*** and **2-Br*** in the gas phase. (b) Kohn−Sham orbitals representing the electronic configuration description of S_1, T_1, and T_2 manifolds of **2-H*** (b) and **2-Br*** (c). Indicated percentages describe the overall character for each displayed transition.

To obtain transient photoluminescence lifetime measurements, a sample was placed in a quartz tube (6 mm outer diameter, 4 mm inner diameter) and sealed with a small septum. The solution was then deoxygenated via purging with N_2 gas for about 5 min. A 170 μJ pulsed 337 nm N_2 laser was used as the excitation source with photoluminescence detected using a silicon detector coupled to a 400 nm long-pass optical filter. The resulting time-dependent photoluminescence data were recorded with an oscilloscope. Some residual laser signal is present as the prompt component of these decays and were not considered in our analysis. To extract the lifetime, data past this artificial prompt signal (i.e., after 1 μs) was subjected to a linear fit on the logarithmic scale.

Electronic Structure Calculations. Molecules were built, and molecular mechanics were used to minimize geometries using Avogadro.[40] TD-DFT calculations were performed using the ORCA software package.[41−43] First, geometries were optimized using the AccOpt standard calculation level implemented in ORCA (BP86 functional,[44] ORCA default basis 4: TZVP(2d) for all non-hydrogens, and TZV(p) for hydrogens[45]). Numerical frequencies were then calculated to determine that geometries represented minima on the potential energy surface. Using the optimized geometries, TD-DFT calculations[42] were carried out using the same bases, with the PBE0 functional[46] and increased grid accuracy, and the resolution of identity chain-of-spheres module, RIJCOSX,[43] was used to reduce the computational cost of the calculations. The first 10 excited state levels and their excitation profiles were calculated for each molecule at the ground state geometry, for both singlet and triplet states, affording a first-order description of the energetic landscape. Electronic configuration descriptions of the relevant excited states (S_1, T_1, and T_2) were visualized using Kohn−Sham orbitals depicted using the Avogadro software with extended ORCA support. All simulated molecules were treated without solvation (i.e., gas phase).

4,7-Dichloro-5,6-bis(tetradecyloxy)benzo[2,1,3]thiadiazole (1-Cl). In an oven-dried two-neck 100 mL round-bottom flask equipped with a magnetic stir bar and condenser were combined 5,6-bis(tetradecyloxy)benzo[2,1,3]thiadiazole[27] (300 mg, 0.535 mmol), N-chlorosuccinimide (157 mg, 1.18 mmol), and anhydrous $CHCl_3$ (30 mL). $FeCl_3$ (101 mg, 0.628 mmol) was added to the stirring solution under a stream of argon. The reaction was stirred under argon at 50 °C for 72 h. The reaction mixture was cooled to room temperature, diluted with 30 mL $CHCl_3$, and poured into 50 mL of H_2O. The organic layer was washed with 100 mL of $NaHCO_3$ (aq) and 100 mL of saturated NaCl (aq), dried with $MgSO_4$, filtered, and evaporated. The brown crude product was subjected to column chromatography (1:1 $CHCl_3$/hexanes) to furnish **1-Cl** as a white solid (117 mg, 35% yield). R_f = 0.38 (SiO_2 TLC, 1:1 $CHCl_3$/hexanes). ^{1}H NMR (400 MHz, $CDCl_3$): δ 4.18 (t, J = 6.7 Hz, 4H), 1.87 (m, 4H), 1.53 (m, 4H), 1.40−1.26 (m, 40H), 0.88 (t, J = 7.0 Hz, 6H). ^{13}C NMR (101 MHz, $CDCl_3$): δ 153.3, 149.8, 116.4, 75.4, 32.1, 30.4, 29.86, 29.85, 29.84, 29.82, 29.79, 29.76, 29.6, 29.5, 26.1, 22.9, 14.3. HRMS (ESI): m/z calcd for $C_{34}H_{58}Cl_2N_2O_2S$ $[M + H]^+$ 629.3669, found 629.3687.

4,7-Dibromo-5,6-bis(tetradecyloxy)benzo[2,1,3]thiadiazole (1-Br). Compound **1-Br** was synthesized as reported by Bouffard and Swager,[27] but with modified purification. To a 50 mL round-bottom flask equipped with magnetic stirbar were combined 5,6-bis(tetradecyloxy)-benzo[2,1,3]thiadiazole (300 mg, 0.535 mmol), CH_2Cl_2 (15 mL), and AcOH (7 mL). To this solution was added Br_2 (528 mg, 0.169 mmol, 0.17 mL) dropwise. The flask was stoppered and wrapped with aluminum foil, and the contents were stirred for 2 days. The reaction mixture was then poured into 50 mL of 5% w/v $Na_2S_2O_3 \cdot 5H_2O$ (aq) and washed. The organic layer was then washed with 2 × 50 mL saturated $NaHCO_3$ (aq) and 50 mL saturated NaCl (aq), dried with $MgSO_4$, filtered, and evaporated. The crude residue was subjected to column

chromatography (3:7 CHCl$_3$/hexanes) to yield **1-Br** as a white solid (244 mg, 64% yield). Characterization data are consistent with those already reported. ^{1}H NMR (400 MHz, CDCl$_3$): δ 4.16 (t, J = 6.7 Hz, 4H), 1.88 (m, 4H), 1.53 (m, 4H), 1.38–1.26 (m, 40H), 0.88 (t, J = 7.0 Hz, 6H).

5,6-Bis(hexadecylthio)benzo[2,1,3]thiadiazole (2-H). To a 25 mL Schlenk flask equipped with a magnetic stirbar were added 5,6-dibromobenzo[2,1,3]thiadiazole (350 mg, 1.19 mmol), Pd$_2$dba$_3$ (27.3 mg, 29.8 μmol), and XantPhos (34.5 mg, 59.3 μmol). The flask was then evacuated and backfilled with argon three times before addition of anhydrous toluene (6 mL), diisopropylethylamine (2 mL), and 1-hexadecanethiol (954 mg, 1.14 mL, 3.69 mmol). After being purged with argon for 15 min at room temperature, the reaction mixture was stirred at 80 °C under argon for 19 h. The reaction mixture was then cooled to room temperature and filtered. Volatiles were then evaporated in vacuo. The crude residue was dissolved in CH$_2$Cl$_2$ and combined with 3 g of silica gel. After removal of the solvent, the solid mixture was dry-loaded onto a silica gel column, and the product was eluted out with 1:1 CH$_2$Cl$_2$/hexanes. The recovered product was last recrystallized from isopropanol to obtain pure **2-H** as a light yellow solid (623 mg, 81% yield). R_f = 0.49 (SiO$_2$ TLC, 1:1 CH$_2$Cl$_2$/hexanes). ^{1}H NMR (400 MHz, CDCl$_3$): δ 7.68 (s, 2H), 3.04 (t, J = 7.4 Hz, 4H), 1.79 (m, 4H), 1.50 (m, 4H), 1.35–1.25 (m, 48H), 0.87 (t, J = 7.0 Hz, 6H). ^{13}C NMR (101 MHz, CDCl$_3$): δ 153.4, 142.3, 116.0, 33.6, 32.1, 29.84, 29.81, 29.78, 29.7, 29.6, 29.5, 29.33, 29.25, 28.2, 22.8, 14.3. HRMS (DART): m/z calcd for C$_{38}$H$_{68}$N$_2$S$_3$ [M + H]$^+$ 649.4617, found 649.4617.

4,7-Dibromo-5,6-bis(hexyldecylthio)benzo[2,1,3]thiadiazole (2-Br). In a 50 mL round-bottom flask equipped with a magnetic stirbar was dissolved **2-H** (100 mg, 0.154 mmol) in a mixture of CH$_2$Cl$_2$ (15 mL) and AcOH (4 mL) and chilled to 0 °C. To the stirring suspension was added I$_2$ (1.75 mg, 7.70 μmol) followed by Br$_2$ (123 mg, 0.770 mmol, 0.04 mL) dropwise. The contents were warmed to room temperature and stirred in the dark for 48 h. The reaction mixture was then poured into 50 mL of 5% w/v Na$_2$S$_2$O$_3$·5H$_2$O (aq) and washed with 50 mL of saturated NaHCO$_3$ (aq) and 50 mL saturated NaCl (aq). The organic layer was dried with MgSO$_4$ and filtered. Volatiles were evaporated, and the crude residue was purified by column chromatography (3:7 CHCl$_3$/hexanes) to obtain **2-Br** as a light yellow solid (79 mg, 64% yield). R_f = 0.31 (SiO$_2$ TLC, 3:7 CHCl$_3$/hexanes). ^{1}H NMR (400 MHz, CDCl$_3$): δ 3.08 (t, J = 7.4 Hz, 4H), 1.61 (m, 4H), 1.42 (m, 4H), 1.25–1.24 (m, 48H), 0.88 (t, J = 7.0 Hz, 6H). ^{13}C NMR (101 MHz, CDCl$_3$): δ 153.0, 144.5, 122.6, 38.4, 32.1, 29.84, 29.82, 29.81, 29.79, 29.73, 29.65, 29.5, 29.3, 29.0, 22.8, 14.3. HRMS (DART): m/z calcd for C$_{38}$H$_{66}$Br$_2$N$_2$S$_3$ M$^+$ 806.2741, found 806.2734.

ASSOCIATED CONTENT

Ⓢ Supporting Information

The Supporting Information is available free of charge on the ACS Publications website at DOI: 10.1021/acs.joc.6b00789.

^{1}H and ^{13}C NMR spectra and computational data (PDF)

AUTHOR INFORMATION

Corresponding Author

*E-mail: tswager@mit.edu.

Notes

The authors declare no competing financial interest.

ACKNOWLEDGMENTS

REFERENCES

(1) Müllen, K.; Scherf, U. *Organic Light Emitting Devices: Synthesis, Properties, and Applications*; Wiley–VCH: Hoboken, NJ, 2006.

(2) Yersin, H. *Highly Efficient OLEDs with Phosphorescent Materials*; Wiley–VCH: Hoboken, NJ, 2008.

(3) Evans, R. C.; Douglas, P.; Winscom, C. J. *Coord. Chem. Rev.* **2006**, *250*, 2093–2126.

(4) (a) Yogo, T.; Urano, Y.; Ishitsuka, Y.; Maniwa, F.; Nagano, T. *J. Am. Chem. Soc.* **2005**, *127*, 12162–12163. (b) Zhang, C.; Zhao, J.; Wu, S.; Wang, Z.; Wu, W.; Ma, J.; Guo, S.; Huang, L. *J. Am. Chem. Soc.* **2013**, *135*, 10566–10578. (c) Kamkaew, A.; Lim, S. H.; Lee, H. B.; Kiew, L. V.; Chung, L. Y.; Burgess, K. *Chem. Soc. Rev.* **2013**, *42*, 77–88. (d) Zhao, J.; Wu, W.; Sun, J.; Guo, S. *Chem. Soc. Rev.* **2013**, *42*, 5323–5351.

(5) (a) Horie, K.; Mita, I. *Chem. Phys. Lett.* **1982**, *93*, 61–65. (b) Horie, K.; Morishita, K.; Mita, I. *Macromolecules* **1984**, *17*, 1746–1750.

(6) Lee, D.; Bolton, O.; Kim, B. C.; Youk, J. H.; Takayama, S.; Kim, J. *J. Am. Chem. Soc.* **2013**, *135*, 6325–6329.

(7) Hirata, S.; Totani, K.; Zhang, J.; Yamashita, T.; Kaji, H.; Marder, S. R.; Watanabe, T.; Adachi, C. *Adv. Funct. Mater.* **2013**, *23*, 3386–3397.

(8) Kwon, M. S.; Lee, D.; Seo, S.; Jung, J.; Kim, J. *Angew. Chem., Int. Ed.* **2014**, *53*, 11177–11181.

(9) Lee, D.; Jung, J.; Bilby, D.; Kwon, M. S.; Yun, J.; Kim, J. *ACS Appl. Mater. Interfaces* **2015**, *7*, 2993–2997.

(10) Ramamurthy, V.; Caspar, J. V.; Eaton, D. F.; Kuo, E. W.; Corbin, D. R. *J. Am. Chem. Soc.* **1992**, *114*, 3882–3892.

(11) Yuan, W. Z.; Shen, X. Y.; Zhao, H.; Lam, J. W. Y.; Tang, L.; Lu, P.; Wang, C.; Liu, Y.; Wang, Z.; Zheng, Q.; Sun, J. Z.; Ma, Y.; Tang, B. Z. *J. Phys. Chem. C* **2010**, *114*, 6090–6099.

(12) Bolton, O.; Lee, K.; Kim, H.-J.; Lin, K. Y.; Kim, J. *Nat. Chem.* **2011**, *3*, 207–212.

(13) Bolton, O.; Lee, D.; Jung, J.; Kim, J. *Chem. Mater.* **2014**, *26*, 6644–6649.

(14) Gao, H. Y.; Shen, Q. J.; Zhao, X. R.; Yan, X. Q.; Pang, X.; Jin, W. J. *J. Mater. Chem.* **2012**, *22*, 5336–5343.

(15) Yang, Z.; Mao, Z.; Zhang, X.; Ou, D.; Mu, Y.; Zhang, Y.; Zhao, C.; Liu, S.; Chi, Z.; Xu, J.; Wu, Y.-C.; Lu, P.-Y.; Lien, A.; Bryce, M. R. *Angew. Chem., Int. Ed.* **2016**, *55*, 2181–2185.

(16) Ventura, B.; Bertocco, A.; Braga, D.; Catalano, L.; d'Agostino, S.; Grepioni, F.; Taddei, P. *J. Phys. Chem. C* **2014**, *118*, 18646–18658.

(17) Bergamini, G.; Fermi, A.; Botta, C.; Giovanella, U.; Di Motta, S.; Negri, F.; Peresutti, R.; Gingras, M.; Ceroni, P. *J. Mater. Chem. C* **2013**, *1*, 2717–2724.

(18) Fermi, A.; Bergamini, G.; Roy, M.; Gingras, M.; Ceroni, P. *J. Am. Chem. Soc.* **2014**, *136*, 6395–6400.

(19) Fermi, A.; Bergamini, G.; Peresutti, R.; Marchi, E.; Roy, M.; Ceroni, P.; Gingras, M. *Dyes Pigm.* **2014**, *110*, 113–122.

(20) He, G.; Torres Delgado, W.; Schatz, D. J.; Merten, C.; Mohammadpour, A.; Mayr, L.; Ferguson, M. J.; McDonald, R.; Brown, A.; Shankar, K.; Rivard, E. *Angew. Chem.* **2014**, *126*, 4675–4679.

(21) He, G.; Wiltshire, B. D.; Choi, P.; Savin, A.; Sun, S.; Mohammadpour, A.; Ferguson, M. J.; Farsinezhad, S.; Brown, A.; Shankar, K.; Rivard, E. *Chem. Commun.* **2015**, *51*, 5444–5447.

(22) Xu, J.; Takai, A.; Kobayashi, Y.; Takeuchi, M. *Chem. Commun.* **2013**, *49*, 8447–8449.

(23) Donkerbroek, J. J.; Elzas, J. J.; Gooijer, C.; Frei, R. W.; Velthorst, N. H. *Talanta* **1981**, *28*, 717–723.

(24) Koch, M.; Perumal, K.; Blacque, O.; Garg, J. A.; Saiganesh, R.; Kabilan, S.; Balasubramanian, K. K.; Venkatesan, K. *Angew. Chem., Int. Ed.* **2014**, *53*, 6378–6382.

(25) (a) Scypinski, S.; Love, L. J. C. *Anal. Chem.* **1984**, *56*, 322–327. (b) Hamai, S. *J. Chem. Soc., Chem. Commun.* **1994**, 2243–2244. (c) de la Pena, A. M.; Salinas, F.; Gomez, M. J.; Sanchez-Pena, M.; Duran-Meras, I. *Talanta* **1993**, *40*, 1657–1664.

(26) Neto, B. A. D.; Lapis, A. A. M.; da Silva Júnior, E. N.; Dupont, J. *Eur. J. Org. Chem.* **2013**, *2013*, 228–255.

(27) Bouffard, J.; Swager, T. M. *Macromolecules* **2008**, *41*, 5559–5562.

(28) Gutierrez, G. D.; Coropceanu, I.; Bawendi, M. G.; Swager, T. M. *Adv. Mater.* **2016**, *28*, 497–501.

(29) While there have been many reports on the synthesis and use of **1-Br** and its alkylated derivatives, no reports of red phosphorescence from this type of structure have previously been presented. Additionally, there are no previous reports of **1-I** or known alkylated derivatives exhibiting phosphorescence. We note that the application of column chromatography to all molecules presented in this study removes impurities that obscure clear observations of phosphorescence.

(30) The synthesis of a benzo[2,1,3]thiadiazole functionalized with alkyl thioethers at the 4 and 7 positions has been reported. See: Liu, X.-Y.; Usui, T.; Hanna, J. *Chem. - Eur. J.* **2012**, *20*, 14207−14212.

(31) Itoh, T.; Mase, T. *Org. Lett.* **2004**, *6*, 4587−4590.

(32) Heinrich, G.; Schoof, S.; Gusten, H. J. *J. Photochem.* **1974**, *3*, 315−320.

(33) Kasha, M. *Discuss. Faraday Soc.* **1950**, *9*, 14−19.

(34) Turro, N. J.; Ramamurthy, V.; Scaiano, J. C. *Modern Molecular Photochemistry of Organic Molecules*; University Science Books: Sausalito, CA, 2010.

(35) El-Sayed, M. A. *J. Chem. Phys.* **1965**, *43*, 2864−2872.

(36) The alkyl chain was additionally changed to propyl to account for the very large electron density contributions from the sulfur atoms of the thioethers within the calculated occupied molecular orbitals.

(37) (a) El-Sayed, M. A. *J. Chem. Phys.* **1962**, *36*, 573−574. (b) El-Sayed, M. A. *J. Chem. Phys.* **1963**, *38*, 2834−2838.

(38) Because our calculations were carried out in the gas phase, the deviation of the calculated S_1 state (2.60 eV; λ = 477 nm) from experimental data ($\lambda \sim$ 400−420 nm) for **2-Br** could largely be the result of a significant hypsochromic shift commonly exhibited by n→π* transitions upon solvation. Although smaller, such a deviation is also observed for the S_1 state of **2-H** (calculated wavelength for S_1: 402 nm; observed: 382 nm). See: Karelson, M.; Zerner, M. C. *J. Am. Chem. Soc.* **1990**, *112*, 9405−9406.

(39) Brouwer, A. M. *Pure Appl. Chem.* **2011**, *83*, 2213−2228.

(40) Hanwell, M. D.; Curtis, D. E.; Lonie, D. C.; Vandermeersch, T.; Zurek, E.; Hutchison, G. R. *J. Cheminf.* **2012**, *4*, 17.

(41) Neese, F. *Wiley Interdiscip. Rev. Comput. Mol. Sci.* **2012**, *2*, 73−78.

(42) Petrenko, T.; Krylova, O.; Neese, F.; Sokolowski, M. *New J. Phys.* **2009**, *11*, 015001.

(43) Neese, F.; Wennmohs, F.; Hansen, A.; Becker, U. *Chem. Phys.* **2009**, *356*, 98−109.

(44) (a) Becke, A. D. *Phys. Rev. A: At., Mol., Opt. Phys.* **1988**, *38*, 3098−3100. (b) Perdew, J. P. *Phys. Rev. B: Condens. Matter Mater. Phys.* **1986**, *33*, 8822−8824.

(45) (a) Schäfer, A.; Horn, H.; Ahlrichs, R. *J. Chem. Phys.* **1992**, *97*, 2571−2577. (b) Weigend, F.; Ahlrichs, R. *Phys. Chem. Chem. Phys.* **2005**, *7*, 3297−3305.

(46) Adamo, C.; Barone, V. J. *J. Chem. Phys.* **1999**, *110*, 6158−6169.